

## BLOOD FLOW IN MICROVESSELS

Y.G. Stergiou<sup>1</sup>, A.T. Keramydas<sup>1</sup>, A.D. Anastasiou<sup>2</sup>, S.V. Paras<sup>1\*</sup>

<sup>1</sup>Chemical Engineering Dept., Aristotle University of Thessaloniki, Greece

<sup>2</sup>School of Chemical and Process Engineering, University of Leeds, UK

(\*paras@auth.gr)

### ABSTRACT

The study of hemodynamics is particularly important in medicine and biomedical engineering as it is crucial for the design of new implantable devices and for understanding the mechanism of various diseases related with blood flow. In this study we measure the plasma *Cell Free Layer (CFL)* which is the result of *Fahraeus-Lindqvist* effect. To achieve it, the test section is illuminated by a light source placed under the microchannel and the flow is recorded with a high-speed camera. It is observed that the width of the *CFL* increases as the diameter of the tube is increased and decreases as the hematocrit ( $H_{ct}$ ) is increased. Based on the experimental results we propose a correlation for the prediction of the *CFL* width as a function of Reynolds number ( $Re_{\infty}$ ) and  $H_{ct}$ . This correlation was used in a “two-fluids” computational model to describe the fluid behavior in microvessels with i.d. less than 300 $\mu$ m. The CFD results are found to be in relative accordance with the experimental data.

### INTRODUCTION

The characteristics of blood flow in small arteries are of great interest for biomedical engineering. The results of such studies will provide information which will be useful in understanding *in vivo* blood flow conditions, in designing medical devices (e.g. organs on a chip) or in the development of more effective diagnostic tools. Blood flow in large arteries has been extensively studied<sup>[1]</sup>. However, little work has been done regarding the blood flow in small vessels, mainly because both *in vivo* and *in vitro* experiments in small arteries are difficult to perform. In an experimental study in our Laboratory, Anastasiou et al.<sup>[2]</sup> used a blood substitute, i.e. a fluid that has the viscoelastic properties of blood, and they conducted experiments in a 600 $\mu$ m i.d. conduit. However, it is well known that in blood vessels with i.d.<300 $\mu$ m the ***Fahraeus-Lindqvist*** effect<sup>[3]</sup> must be also taken into account, i.e. during blood flow in such microvessels the erythrocytes migrate towards the center of the channel resulting to the formation of *CFL* along the vessel wall. The *CFL* width is defined as the distance from the outer edge of the *RBC* core to the luminal surface of the endothelium<sup>[4]</sup>. This effect has been confirmed by both *in-vivo* and *in-vitro* experiments inside glass capillaries<sup>[5,6]</sup>. There are many parameters which affect the *CFL*, namely the diameter of the vessel, the  $H_{ct}$  and the flow conditions which can be described either by  $Re_{\infty}$  or as it can be found in many studies<sup>[7]</sup> by the pseudo shear rate (defined as mean velocity/vessel diameter). As expected, the *CFL* exhibits a lower viscosity than the rest of the fluid and this facilitates the blood flow through the microvessels. Although this phenomenon is significant for diameters< 300 $\mu$ m most of the published work<sup>[5]</sup> is focused on vessel diameters between 20-100 $\mu$ m.

Motivated by the importance of these parameters in biomedical engineering the aim of this study is twofold. The first one is to estimate the *CFL* extent. In this study, we investigate the effect of  $Re_{\infty}$  and  $H_{ct}$  on *CFL* characteristics in three microvessels with 50, 100 and 170 $\mu$ m hydraulic diameter. The experimental data will be used for formulating a correlation for estimating the *CFL* width under various flow conditions. The second one is to utilize the outcome of the experimental part in order to develop a simplified “two-phase” model using Computational Fluid Dynamics (*CFD*), a common

practice in literature<sup>[8]</sup>. The *CFL* flow domain will be solved assuming the blood properties are that of a Newtonian fluid, whereas in the vessel core the blood rheology is formulated using a non-Newtonian model. Simulations will be executed for various blood velocities and various vessel diameters. The blood flow characteristics and patterns will be calculated, as well as the Wall Shear Stress (*WSS*) magnitude and the overall Pressure Drop ( $\Delta P$ ) across the vessels, to elucidate the phenomena of the cases studied experimentally.

## EXPERIMENTAL PROCEDURE

The fluids used for our experiments were mixtures of red blood cells (*RBC*) and physical saline whose physical properties were found to be like those of blood. A small amount of *EDTA* prevents coagulation, thus, we can assume that the extent of cell aggregation is similar to that of a healthy man. The *RBCs* were collected from healthy adult volunteers and the process of purification comprises the following steps:

- Centrifugation (at 3200rpm) is performed in the whole blood sample for the separation of erythrocytes from plasma.
- The separated red blood cells are washed with saline water and are twice recentrifugated.

The acquired *RBCs* are then used to produce “blood” of known  $H_{ct}$ . The compositions of all fluids used in our experiments are presented in **Table 1**. Viscosity measurements were performed using a cone plate rheometer (*AR-G2*, *TA Instruments*) at 24°C. To verify the similarity with “real” blood the *Quemada* model (**Eq. 1**)<sup>[9]</sup> was used for comparison with our *RBC* solutions:

$$\mu = \frac{\mu_p}{(1 - 0.5 \cdot k \cdot H_{ct})^2} \quad (1)$$

$$\text{where } k = \frac{k_0 + k_\infty \cdot \sqrt{\gamma_r}}{1 + \gamma_r} \quad (2)$$

$$\text{and } \gamma_r = \frac{\gamma}{\gamma_c} \quad (3)$$

where  $k_0$ ,  $k_\infty$  and  $\gamma_c$  are, in general, functions of *RBC* concentration.

**Table 1:** Fluids composition (%v/v).

	<i>RBC</i>	<i>Saline</i>	<i>EDTA</i>
$H_5$	5	94.5	0.5
$H_{10}$	10	89.5	0.5
$H_{20}$	20	79.5	0.5
$H_{30}$	30	69.5	0.5
$H_{40}$	40	59.5	0.5

The comparison between the *Quemada* model and the experimental data showed that the fluids used exhibit non-Newtonian behavior and can be used in experiments that simulate blood. *RBCs* have the property of absorbing light and the measuring technique of *CFL* is based on this fact. Placing a light source at the bottom of the micro channel and recording the flow from above with a high speed camera, we were able to identify on the recorded images the areas of low *RBC* concentration, i.e. brighter areas (**Fig. 1**). All experiments were conducted in three channels with square cross section (50x50, 170x170 & 100x100 $\mu\text{m}$ ), etched on a *PMMA* plate and sealed with the same material.

## CFL MEASUREMENTS

The first objective of this study is to investigate the parameters that affect the size of the *CFL*. We

performed experiments with RBC solutions with  $H_{ct}$  10, 20, 30 and 40% and  $Re_{\infty}$  0.3-6. It must be noted that for calculating the  $Re_{\infty}$ , as *reference* viscosity was used the one obtained from the *Quemada* model for very high shear rates ( $\dot{\gamma} > 1000 \text{ s}^{-1}$ ). The effect of the channel diameter on the CFL was investigated by conducting experiments in three microchannels with hydraulic diameters of 50, 100 and 170  $\mu\text{m}$ . We have measured the CFL at steady state conditions by acquiring and analyzing an appropriate number of consecutive frames and then we used the data for constructing the CFL traces and for calculating the average CFL width (**Fig. 2**).

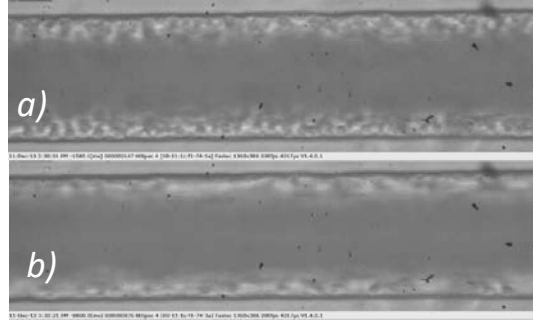


**Figure 1.** Typical images for: a)  $Q=0.5 \text{ ml/hr}$  and b)  $Q=1.2 \text{ ml/hr}$ . ( $D=100 \mu\text{m}$ ,  $H_{ct}=20\%$ ).

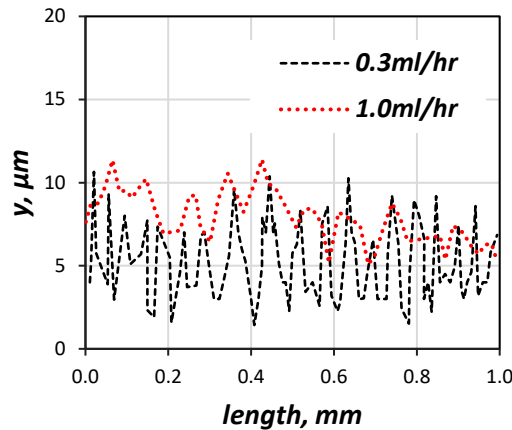


**Figure 2.** Typical CFL traces for  $Q=0.1 \text{ ml/h}$  and  $Q=1.5 \text{ ml/hr}$ ;  $H_{ct}=20\%$ ,  $D=100 \mu\text{m}$  (wall  $y=0$ ).

The results showed that the CFL normalized with respect to the hydraulic diameter,  $CFL/D$ , decreases with increasing  $H_{ct}$ , an observation in accordance with Namgung et al.<sup>[5]</sup> This outcome is due to the fact that as the concentration of the RBCs increases, the viscous forces increase and hinder the movement of the cells in the middle of the channel. Additionally, it seems that the normalized CFL decreases as the diameter of the microchannel increases, a fact that is also confirmed by Namgung et al.<sup>[5]</sup> The results also showed that in the flow rate range where migration started, there is still a low cell concentration near the wall and not a total absence of cells.

The CFL measurements for several volumetric flow rates revealed that when the flow rate is low and CFL starts to be formed, there is a small increase rate of CFL until it reaches a constant value for  $Re_{\infty} > 4$ . This can be explained as follows. As the RBCs are migrating towards the center of the vessel their concentration increases up to a point that the viscous forces hinder additional migration. Using Response Surface Methodology (RSM) a 2<sup>nd</sup> order polynomial equation, also known as quadratic model (Eq. 4), which calculates the normalized CFL is formulated:

$$\frac{CFL}{D} = a_0 + a_1 H_{ct} + a_2 Re_{\infty} + a_3 H_{ct}^2 + a_4 Re_{\infty}^2 + a_5 H_{ct} Re_{\infty} \quad (4)$$

The equation formulated in the present study (Eq. 4) calculates  $CFL/D$  as a function of  $Re_{\infty}$  and  $H_{ct}$ . The coefficients (Table 1) are determined using the experimental data for two ( $k=2$ ) variables.

Predictions of the proposed correlation was checked with the limited available in the literature experimental data<sup>[7]</sup> and are found to be in good agreement (**Fig. 4**).

**Table 1.** Coefficients of the CFL correlation

$\alpha_0$	0.066384	$\alpha_3$	0.000002
$\alpha_1$	-0.000887	$\alpha_4$	-0.001414
$\alpha_2$	0.017796	$\alpha_5$	-0.000005

**Eq. 4** gives accurate results for  $Re_\infty$  between 0.3-6 and  $H_{ct}$  5-40% with an uncertainty of 10%. The accuracy of the equation was calculated by comparing the correlation with the experimental results. It seems that this correlation predicts the behavior of the CFL as described previously. For  $Re_\infty > 4$  the CFL/D is approaching a constant value which depends on the  $H_{ct}$ .

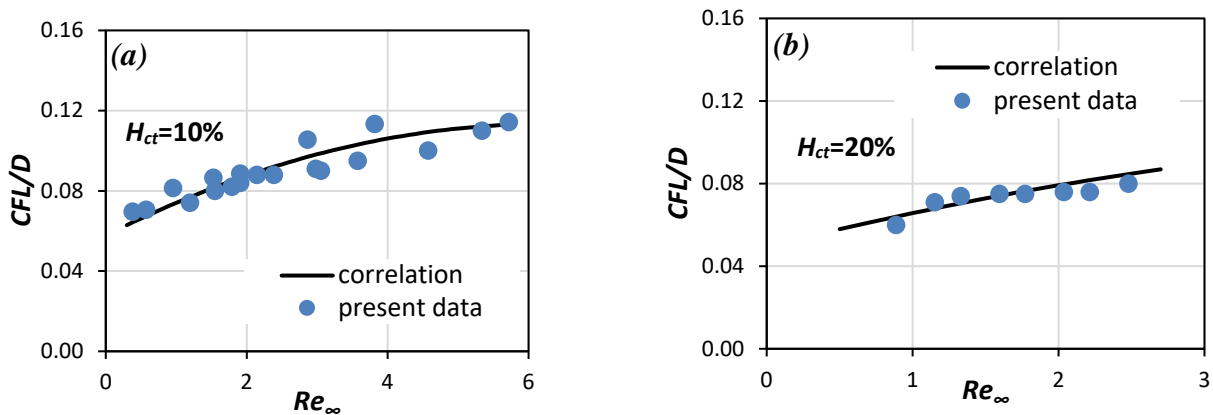


**Figure 3.** Comparison of correlation with CFL experimental data for: a)  $H_{ct}=10\%$  and b)  $H_{ct}=20\%$ .

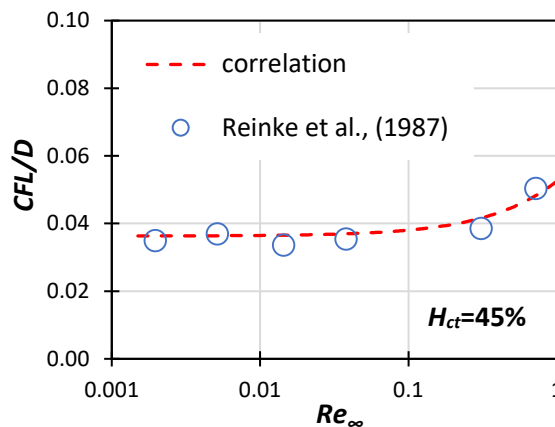


**Figure 4.** Comparison of correlation with Reinke et al.<sup>[7]</sup> data.

### CFD SIMULATIONS

In our simulations the Fahraeus effect<sup>[10]</sup> was taken into consideration and was modelled using a relative correlation<sup>[11]</sup>. Moreover, the lateral variation of the  $H_{ct}$  in the core area was modelled using the Lih<sup>[12]</sup> model distribution, fitted for each case. The blood density is set at a constant value ( $\rho_b=1050\text{kg/m}^3$ ). Blood is modelled as a Newtonian fluid having the viscosity of human blood plasma ( $\mu_p=1.2\text{cP}$ ) in the CFL zone, whereas, the blood in the core area is modelled as non-Newtonian shear thinning fluid. This is achieved through a modified<sup>[13]</sup> Quemada model where local  $\mu$  is expressed by **Eq. 1**,  $K$  is expressed by **Eq. 2** and its coefficients ( $k_0, k_\infty, \gamma_C$ ) are expressions of  $H_{ct}$  obtained by Das et al.<sup>[13]</sup>. CFD modeling in this study was conducted using the ANSYS CFX 19 commercial code.

The blood vessels (Length ( $L$ ), 1mm) were modeled as two-dimensional computational domains with axial symmetry and an adjustable radius ( $R$ ). The geometry of the domain and the mesh were designed on ANSYS Workbench package (v. 19). As  $Re_\infty$  numbers are low, the flow is laminar. Thus, the Direct Numerical Simulation (DNS) model was used while the high-resolution advection scheme was employed for the discretization of the momentum equations. The simulations were run in a steady state, the vessel walls were considered smooth and a no-slip boundary condition was employed. As for the meshing procedure, an optimum grid density was chosen by performing a grid dependency study. Consequently, cells with a maximum face size of  $2.5\mu\text{m}$  were used, while mesh refinement was applied in areas where viscosity changes were pronounced.

Simulations were performed for diameters varying between 80 and  $170\mu\text{m}$ ,  $H_{ct}$  between 30% and 50% and,  $Re_\infty$  between 0.8 and 4.9. The parameters were mainly selected depending on the availability of previous literature *in vitro* velocity experiments, so that the results could be contrasted and juxtaposed with the literature data<sup>[14]</sup>. In **Fig. 5**, the blood viscosity magnitude is illustrated for one of the cases tested ( $D=100\mu\text{m}$ ,  $Re_\infty=0.8$ ,  $H_{ct}=30\%$ ). The CFL zone is depicted, where the viscosity is that of blood plasma, whereas in the non-Newtonian core the viscosity gradually decreases as radial distance increases. The comparison of the flow patterns of our simulation with relative experimental data are used as a form of code validation. In **Fig. 6** the axial velocity distribution of one case ( $D=80\mu\text{m}$ ,  $Re_\infty=0.3$ ,  $H_{ct}=37\%$ ) are associated with experimental measurements by Gaehtgens et al.<sup>[14]</sup> There seems to be a relatively good accordance of experimental and computational results, bound with a deviation of 10%. The main problems (as shown in **Fig. 6**) appear near the boundary between the core and the CFL.

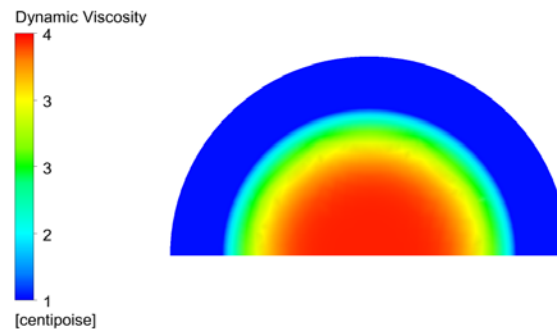


**Figure 5.** Graphical representation of the viscosity distribution on a cross section ( $Re_\infty=0.8$ ,  $H_{ct}=30\%$ ).

The overall  $\Delta P_{CFL}$  was calculated across the whole length of the vessel and was compared with two values: the  $\Delta P_D$  calculated analytically using the Darcy law for straight circular tubes and considering the blood as a Newtonian fluid ( $\mu_b=3.5\text{cP}$ ) and the  $\Delta P_{nCFL}$  calculated numerically considering that the CFL is completely absent and that the blood behaves as a non-Newtonian fluid (in the same way the non-Newtonian core was modelled previously). Typical results for some of the cases tested are summarized in **Table 2**. As presented in **Table 2**, omitting to consider the existence of CFL, in vessels that the *Fahraeus-Lindqvist* effect occurs, leads to significantly **higher** pressure drop.

**Table 2.** Pressure drop for various cases.

$Re_\infty$	$D(\mu\text{m})$	$H_{ct}(\%)$	$\Delta P_{CFL}$ (Pa)	$\Delta P_{nCFL}$ (Pa)	$\Delta P_D$ (Pa)	$\Delta P_{nCFL} / \Delta P_{CFL}$
0.8	100	30	132	238	302	1.8
1.4	170	40	42	103	105	2.5
2.5	170	40	105	187	186	1.8
4.9	170	40	204	377	372	1.8

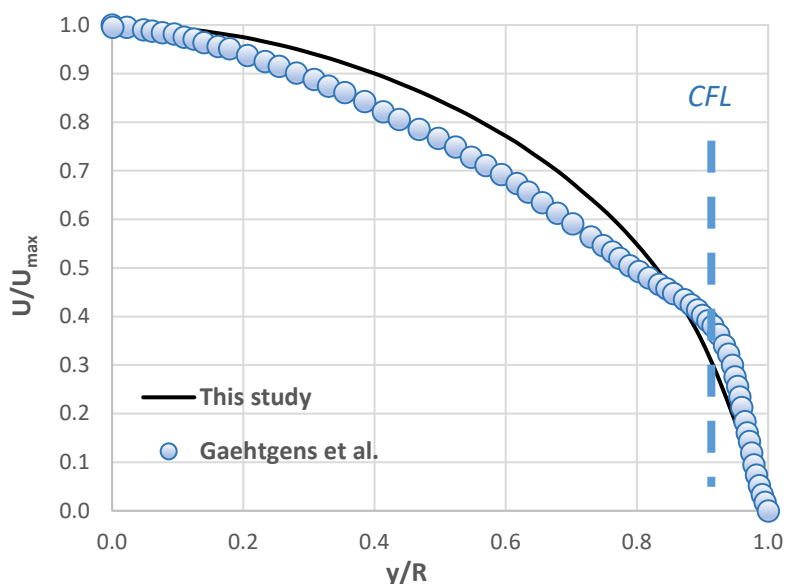


**Figure 6.** Comparison of calculated axial velocity and axial velocity obtained by Gaehtgens et al.<sup>[14]</sup>

## CONCLUSIONS

The *CFL* width, which is a function of  $Re_\infty$  and  $H_{ct}$  tends to a constant value, which in turn is also affected by the concentration of the *RBCs*. A correlation for predicting  $CFL/D$  has been proposed and its validity has been checked both with the present results and the limited published experimental data. Additionally, the CFD simulations revealed that the proposed correlation for predicting the *CFL* thickness can be used as an input in numerical simulations. Lastly, the importance of including a *CFL* modelling technique in CFD simulations lies on the fact it greatly affects the predicted pressure drop values in such vessels (as much as 2-3 greater in methods without a *CFL* modelling).

## REFERENCES

- [1] R.F. Tuma, W.N. Duran, K. Ley, *Microcirculation*, Academic Press, 2011.
- [2] A.D. Anastasiou, A.S. Spyrogianni, K.C. Koskinas, G.D. Giannoglou, S.V. Paras, *Med. Eng. Phys.* 34 (2012) 211–218.
- [3] R. Fåhræus, T. Lindqvist, *Am. J. Physiol.-Leg. Content* 96 (1931) 562–568.
- [4] P.K. Ong, B. Namgung, P.C. Johnson, S. Kim, *Am. J. Physiol. - Heart Circ. Physiol.* 298 (2010) 1870–1878.
- [5] B. Namgung, M. Ju, P. Cabrales, S. Kim, *Microvasc. Res.* 85 (2013) 68–76.
- [6] A.R. Pries, D. Schönfeld, P. Gaehtgens, M.F. Kiani, G.R. Cokelet, *Am. J. Physiol. - Heart Circ. Physiol.* 272 (1997) 2716–2725.
- [7] W. Reinke, P. Gaehtgens, P.C. Johnson, *Am. J. Physiol.* 253 (1987) H540-547.
- [8] M. Sharan, A.S. Popel, *Biorheology* 38 (2001) 415–428.
- [9] S. Kim, R.L. Kong, A.S. Popel, M. Intaglietta, P.C. Johnson, *Am. J. Physiol. Heart Circ. Physiol.* 293 (2007) 1526-1535.
- [10] R. Fåhræus, *Physiol. Rev.* 9 (1929) 241–274.
- [11] A.R. Pries, T.W. Secomb, P. Gaehtgens, J.F. Gross, *Circ. Res.* 67 (1990) 826–834.
- [12] M.M. Lih, *Bull. Math. Biophys.* 31 (1969) 143–157.
- [13] B. Das, P.C. Johnson, A.S. Popel, *Biorheology* 35 (1998) 69–87.
- [14] P. Gaehtgens, H.J. Meiselman, H. Wayland, *Microvasc. Res.* 2 (1970) 13–23.